FAST APPROXIMATION OF THE LAMBERT W FUNCTION FOR VIRTUAL ANALOG MODELLING

Stefano D'Angelo

Independent researcher
Agropoli, Italy
s@dangelo.audio

Leonardo Gabrielli

Department of Information Engineering,
Università Politecnica delle Marche
Ancona, Italy
l.gabrielli@univpm.it

Luca Turchet

Department of Information Engineering and
Computer Science,
University of Trento
Trento, Italy
luca.turchet@unitn.it

ABSTRACT

When modelling circuits one has often to deal with equations containing both a linear and an exponential part. If only a single exponential term is present or predominant, exact or approximate closed-form solutions can be found in terms of the Lambert W function. In this paper, we propose reformulating such expressions in terms of the Wright Omega function when specific conditions are met that are customary in practical cases of interest. This eliminates the need to compute an exponential term at audio rate. Moreover, we propose simple and real-time suitable approximations of the Omega function. We apply our approach to a static and a dynamic nonlinear system, obtaining digital models that have high accuracy, low computational cost, and are stable in all conditions, making the proposed method suitable for virtual analog modelling of circuits containing semiconductor devices.

1. INTRODUCTION

Typically, circuits are modelled as systems of differential equations which often contain nonlinearities [1, 2]. This is true of both state-space methods [3, 4] and wave digital filters [5, 6, 7]. Because of the exponential relation in the Shockley model of p-n junctions in semiconductors [8], which is also used in the Ebers-Moll model of bipolar junction transistors (BJT) [9], often one has to deal with equations containing both a linear and an exponential part. These equations may be solved numerically by iterative methods. However, these approaches often result in high computational load and can be problematic in terms of stability and/or accuracy [10, 11].

When only a single exponential term is present or predominant, it is possible to utilize the Lambert W function [12, 13, 14] to analytically solve these equations [15, 16, 17, 18, 19, 20, 21]. When applicable, such an approach brings remarkable advantages. In the context of circuit simulation, it is often the case that the solution only involves the main branch of the W function while its argument contains a time-varying exponential term. Various approximations [22, 23, 24, 25, 26] as well as algorithms [27, 28] have been proposed in the literature for the computation of the W function but, to the best of authors' knowledge, evaluation methods have always been preferred, in the context of real-time music DSP, that trade lower accuracy for higher performance [16, 17, 18, 19, 20].

In this paper, we propose to reformulate expressions involving the main branch of the Lambert W function in terms of the Wright Omega function [29] in the context of virtual analog modelling, which eliminates the need to compute the exponential term usually found in the argument. Moreover, we propose simple approximations that can be used when algorithms already available for a precise evaluation of the Omega function (*e.g.*, [30, 31]) are too demanding from a computational standpoint.

The reminder of the paper is structured as follows. Section 2 describes both the Lambert W and Wright Omega functions. Section 3 presents four approximations of the Wright Omega function. Section 4 reports the application of the proposed approach for two circuits, whereas Section 5 concludes the paper.

2. THE LAMBERT W AND WRIGHT OMEGA FUNCTIONS

In this section we introduce very briefly the Lambert W and Wright Omega functions. Since time-domain circuit simulation most often only involves real quantities, we will limit ourselves to the $\mathbb{R} \to \mathbb{R}$ case, that is the argument is real and not less than $-\frac{1}{e}$ for the Lambert W function and just real for the Wright Omega function.

2.1. The Lambert W function

The Lambert W function is a non-injective function, with two branches in the $\mathbb{R} \to \mathbb{R}$ case, which is defined as the inverse function of

$$f(x) = xe^x, \tag{1}$$

where e^x is the exponential function and $x \geq -\frac{1}{e}$. This can be expressed as

$$x = f^{-1}(xe^x) = W(xe^x). \tag{2}$$

The defining equation for the W function can be derived by substituting $x_0 = xe^x$ into equation 2,

$$x_0 = W(x_0)e^{W(x_0)}, \tag{3}$$

for any $x_0 \geq -\frac{1}{e}$.

$W(x)$ is two-valued for $x \in \left[-\frac{1}{e}, 0\right)$, therefore we will refer to the main branch ($W(x) \geq -1$) as $W_0(x)$ and to the other branch ($W(x) \leq -1$) as $W_{-1}(x)$.

Now we can express the solution of equation

$$e^{ax+b} = cx + d, \tag{4}$$

as

$$x = -\frac{W\left(-\frac{a}{c}e^{b-a\frac{d}{c}}\right)}{a} - \frac{d}{c}, \tag{5}$$

with a and c not null. In particular, if a and c have the same sign, the argument of $W()$ is negative and there are either two (possibly coincident) or no solutions, otherwise the argument is positive, there is one solution, and $W(x) = W_0(x)$.

In circuit modelling, often a and c have opposite sign and are either constants or control-rate expressions, while b or d contain audio-rate components [17, 18, 19, 20, 21]. Therefore, under the previous formulation, not only one needs to compute $W()$, but also the exponential in its argument. In these cases, it is however still possible to more conveniently reformulate the previous expression as

$$x = -\frac{W_0\left(e^{b-a\frac{d}{c}+\log(-\frac{a}{c})}\right)}{a} - \frac{d}{c}. \tag{6}$$

2.2. The Wright Omega function

The Wright Omega function is defined in terms of the Lambert W function as

$$\omega(x) = W_0(e^x), \tag{7}$$

which can obviously be used to express equation 6 as

$$x = -\frac{\omega\left(b - a\frac{d}{c} + \log(-\frac{a}{c})\right)}{a} - \frac{d}{c}. \tag{8}$$

In practice the logarithm is typically a constant or a control-rate expression and $\omega()$ is the only transcendental function to be computed at audio-rate.

3. APPROXIMATIONS AND COMPUTATION

High-precision algorithms have been proposed to compute $\omega()$ [30, 31], yet in the context of real-time music DSP it is usually preferable to trade some accuracy for higher computational efficiency. Indeed, some approximations have been already proposed in [16, 18], even if $\omega()$ was not explicitly mentioned. In this section we propose four approximations with different degrees of accuracy and complexity. Moreover, since two of these approximations presuppose fast computation of logarithm and exponential functions, we also discuss two commonly used approaches for approximating them with a focus on the problem at hand, in case the standard routines supplied for the target platform are not sufficiently efficient.

3.1. Approximations of $\omega(x)$

Several approximations of increasing computational cost are proposed hereby. The plot of $\omega(x)$, in Figure 1(a), suggests that a first, rough approximation can be

$$\omega(x) \approx \omega_1(x) = \max(0, x). \tag{9}$$

One could use a cubic spline to smooth the function around 0 as

$$\omega(x) \approx \omega_2(x) = \begin{cases} 0 & \text{for } x \leq x_1, \\ \alpha x^3 + \beta x^2 + \gamma x + \zeta & \text{for } x_1 < x < x_2, \\ x & \text{for } x \geq x_2. \end{cases} \tag{10}$$

It is sufficient to set the conditions of continuity C^1 to univocally determine the parameters $\alpha, \beta, \gamma, \zeta$ from x_1 and x_2. Optimzing

these last two variables by the least squares method to minimize the absolute error in the range $[-10, 10]$ leads to

$$x_1 = -3.684303659906469,$$
$$x_2 = 1.972967391708859,$$
$$\alpha = 9.451797158780131 \cdot 10^{-3},$$
$$\beta = 1.126446405111627 \cdot 10^{-1},$$
$$\gamma = 4.451353886588814 \cdot 10^{-1},$$
$$\zeta = 5.836596684310648 \cdot 10^{-1}.$$

Such an approximation is non optimal for $x \geq x_2$. Since $W(x)e^{W(x)} = x$, then $\omega(x)e^{\omega(x)} = e^x$, or otherwise $\omega(x) = x - \log(\omega(x))$. This last relation can be used as a successive approximation method (*i.e.*, $\omega_n = x - \log(\omega_{n-1})$) for $x \geq 1$ (the same approach is used in [17]). Applying it to improve the accuracy in the range of interest gives

$$\omega(x) \approx \omega_3(x) = \begin{cases} 0 & \text{for } x \leq x_1, \\ \alpha x^3 + \beta x^2 + \gamma x + \zeta & \text{for } x_1 < x < x_2, \\ x - \log(x) & \text{for } x \geq x_2. \end{cases} \tag{11}$$

Again, $\alpha, \beta, \gamma, \zeta$ are univocally determined from x_1 and x_2 if C^1 continuity is imposed. This time we also take into account that fast approximations for $\log(x)$ exist which are exact for $x = 2^y$ with $y \in \mathbb{Z}$, hence we also ensure that x_2 is a power of 2. Reiterating the optimization process, one gets

$$x_1 = -3.341459552768620,$$
$$x_2 = 8,$$
$$\alpha = -1.314293149877800 \cdot 10^{-3},$$
$$\beta = 4.775931364975583 \cdot 10^{-2},$$
$$\gamma = 3.631952663804445 \cdot 10^{-1},$$
$$\zeta = 6.313183464296682 \cdot 10^{-1}.$$

To further improve the accuracy of such approximation, a Newton-Raphson iteration can be applied

$$\omega_4(x) = \omega_3(x) - \frac{\omega_3(x) - e^{x-\omega_3(x)}}{\omega_3(x) + 1}, \tag{12}$$

even if an approximation is used for the exponential term.

Figure 1(a) shows a plot of the $\omega(x)$ function along the four proposed approximations, while Figure 1(b) shows the distribution of the absolute errors for each of them.

3.2. Approximation of $\log(x)$

The logarithm function can be efficiently approximated by exploiting the IEEE754 representation of floating point numbers [32]. The memory representation of any such number is functionally equivalent to

$$x = S2^E(1 + M), \tag{13}$$

where S is either -1 or $+1$, $E \in \mathbb{Z}$ is called the exponent, and $M \in [0, 1)$ is the mantissa.

In our case we can safely assume that $S = +1$, and by using basic properties of logarithms

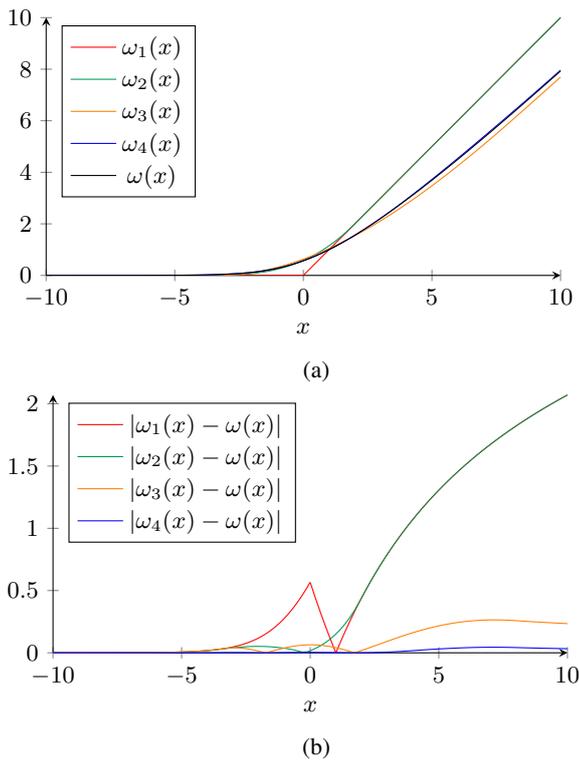$$\log(x) = \frac{1}{\log_2(e)} (E + \log_2(1 + M)). \tag{14}$$

(a)

(b)

Figure 1: *Approximations of the Omega function (a) and their absolute errors (b).*

E can be easily extracted as an integer from the actual floating point representation of x by means of a bitshift and an integer sum, and can be then converted to floating point representation by routines that are usually hardware-provided. Similarly, $1 + M$ can be quickly obtained from x by setting the exponent to 0. Then, $\frac{1}{\log_2(e)}$ is a constant that should just be precomputed and multiplied for the change of base.

Since $1 \le 1 + M < 2$, we have effectively narrowed the problem to the computation of $\log_2(x)$ in this range. We can finally use a cubic spline and impose C^1 continuity on the extremes, thus obtaining

$$\log_2(x) \approx \alpha x^3 + \beta x^2 + \gamma x + \zeta, \qquad (15)$$

with

$$\alpha = 0.1640425613334452,$$
$$\beta = -1.098865286222744,$$
$$\gamma = 3.148297929334117,$$
$$\zeta = -2.213475204444817.$$

3.3. Approximation of e^x

A similar approach can be employed to approximate the exponential function. First, it is possible to express

$$e^x = 2^{\lfloor y \rfloor} 2^{y - \lfloor y \rfloor} \qquad (16)$$

where $y = \frac{1}{\log(2)} x$ can be computed just by a multiplication with a precomputed constant. $2^{\lfloor y \rfloor}$ is also easily obtained in floating

point format by converting y to integer format (usually through fast hardware-implemented routines) and ensuring down rounding is used, then using logic and integer operations so that $S = 1$, $E = \lfloor y \rfloor$, and $M = 0$.

Since $0 \le y - \lfloor y \rfloor < 1$, we have again narrowed the problem to the computation of 2^x in this range. Now $y - \lfloor y \rfloor$ is obtained by converting $\lfloor y \rfloor$ to the floating point format and performing a subtraction, and finally a cubic spline with C^1 continuity on the extremes can be used to get

$$2^x \approx \alpha x^3 + \beta x^2 + \gamma x + \zeta,$$
$$\alpha = 0.07944154167983575,$$
$$\beta = 0.2274112777602189,$$
$$\gamma = 0.6931471805599453,$$
$$\zeta = 1.$$

4. APPLICATIONS

In this section we apply our approach to model two simple circuits, namely a common collector voltage buffer and a dynamic diode clipper, in order to show its suitability for simulating both static and dynamic nonlinear systems.

4.1. Common collector voltage buffer

The common collector configuration is a basic BJT amplifier topology, which is typically used as a voltage buffer. Figure 2 shows the simplest such circuit.
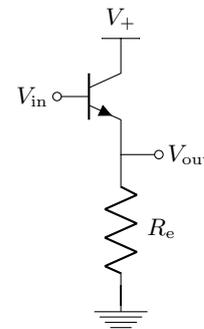

Figure 2: *Diagram of the common collector circuit.*

By examining the emitter node, according to the Ebers-Moll model and Ohm's Law,

$$I_s \left(e^{\frac{V_{in} - V_{out}}{V_T}} - e^{\frac{V_{in} - V_+}{V_T}} + \frac{e^{\frac{V_{in} - V_{out}}{V_T}} - 1}{\beta_f} \right) = \frac{V_{out}}{R_e}, \quad (17)$$

where I_s is the saturation current, V_T is the thermal voltage, and β_f is the common-emitter current gain. This can be solved analyt-

ically in terms of $\omega()$ as

$$V_{\text{out}} = V_{\text{T}}\omega\left(\frac{V_{\text{in}} + V_{\text{x}}}{V_{\text{T}}} + k\right) - V_{\text{x}}, \qquad (18)$$

$$V_{\text{x}} = I_{\text{s}}R_{\text{e}}\left(e^{\frac{V_{\text{in}} - V_{+}}{V_{\text{T}}}} + \frac{1}{\beta_{\text{f}}}\right), \qquad (19)$$

$$k = \log\left(\frac{I_{\text{s}}R_{\text{e}}}{V_{\text{T}}}\left(1 + \frac{1}{\beta_{\text{f}}}\right)\right). \qquad (20)$$

Please note that k is constant and that the exponential in Eq. (19) is directly and solely input-dependent, therefore needing to be computed no matter the modelling method adopted. Moreover, the closed-form solution above is exact, therefore the output error will in practice only be affected by approximations of the $\omega()$ and the exponential functions.

Figure 3 shows the output signals obtained by feeding the proposed model implemented using different $\omega(x)$ approximations with a 9 V_{pp} (Volts peak-to-peak) 440 Hz sine with 4.5 V offset. We have set $V_{+} = 9$ V, $V_{\text{T}} = 26$ mV, $I_{\text{s}} = 0.1$ fA, $\beta_{\text{f}} = 100$, $R_{\text{e}} = 1$ kΩ.

4.2. Diode clipper

The diode clipper is a circuit that prevents the output from exceeding a predefined voltage level. Figure 4 shows a passive, dynamic version of the circuit that also incorporates a first-order lowpass filter. The behavior of the circuit can be fully described by [10]

$$\frac{\text{d}V_{\text{out}}}{\text{d}t} = \frac{V_{\text{in}} - V_{\text{out}}}{RC} - 2\frac{I_{\text{s}}}{C}\sinh\left(\frac{V_{\text{out}}}{V_{\text{T}}}\right), \qquad (21)$$

where I_{s} is the saturation current and V_{T} is the thermal voltage.

The derivative on the left side of the previous equation can be discretized using any linear 1-step method (*e.g.*, trapezoidal rule) as

$$\text{d}V_{\text{out}}[n] = B_0 V_{\text{out}}[n] + B_1 V_{\text{out}}[n-1] - A_1 \text{d}V_{\text{out}}[n-1], \quad (22)$$

where B_0, B_1, A_1 are the coefficients obtained by applying the chosen discretization method. We will also approximate the behavior of the two antiparallel diodes by assuming that, at any time, the forward current of one is much higher than the reverse current of the other [17, 19, 20], which corresponds to substituting $\sinh(x) \approx \frac{1}{2}\text{sgn}(x)\left(e^{|x|} - 1\right)$. Therefore, we obtain

$$B_0 V_{\text{out}}[n] + B_1 V_{\text{out}}[n-1] - A_1 \text{d}V_{\text{out}}[n-1] =$$
$$\frac{V_{\text{in}}[n] - V_{\text{out}}[n]}{RC} - \frac{I_{\text{s}}}{C}\text{sgn}\left(V_{\text{out}}[n]\right)\left(e^{\frac{|V_{\text{out}}[n]|}{V_{\text{T}}}} - 1\right), \qquad (23)$$

which can be analytically solved as

$$V_{\text{out}}[n] = w[n] - V_{\text{T}}r[n]\omega(k_4 r[n]w[n] + k_5), \qquad (24)$$
$$w[n] = k_2 q[n] + k_3 r[n], \qquad (25)$$
$$r[n] = \text{sign}(q[n]), \qquad (26)$$
$$q[n] = k_1 V_{\text{in}}[n] - p[n-1], \qquad (27)$$
$$p[n] = k_6 V_{\text{out}}[n] - A_1 p[n-1], \qquad (28)$$
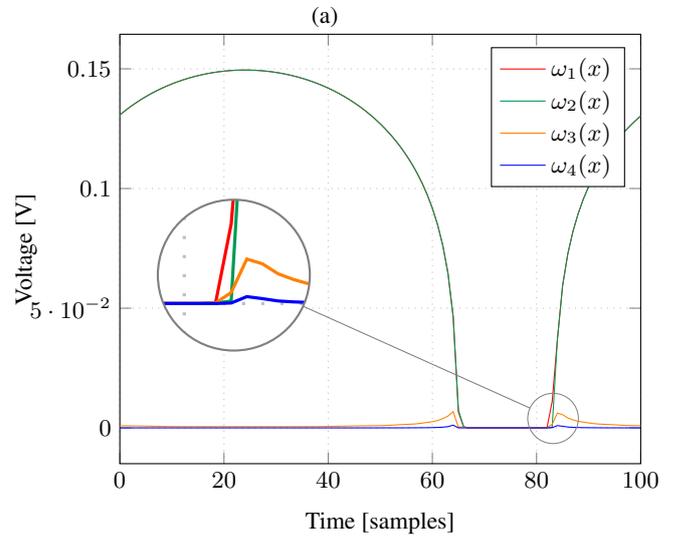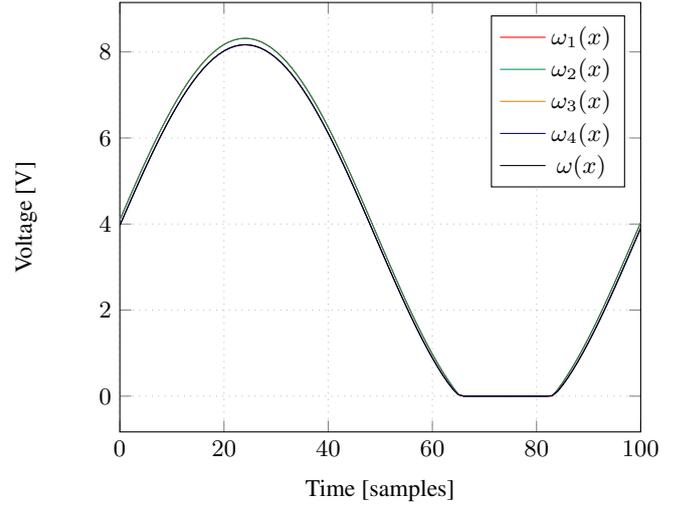

(a)

(b)

Figure 3: *Time domain waveforms (a) and absolute errors (b) of the output from the proposed common collector voltage buffer model implemented using the $\omega(x)$ approximations described in Section 3.1. The input is a 9 V_{pp} 440 Hz sine with 4.5 V offset sampled at 44.1 kHz.*
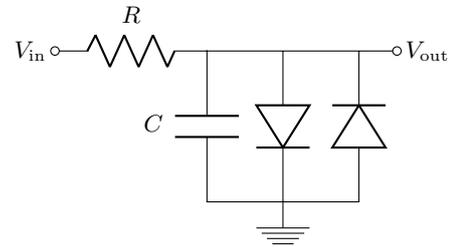

Figure 4: *Diagram of the diode clipper circuit.*

with

$$k_1 = \frac{1}{CR}, \tag{29}$$

$$k_2 = \frac{CR}{B_0 CR + 1}, \tag{30}$$

$$k_3 = \frac{I_s R}{B_0 CR + 1}, \tag{31}$$

$$k_4 = \frac{1}{V_T}, \tag{32}$$

$$k_5 = \log\left(\frac{I_s R}{(B_0 CR + 1)V_T}\right), \tag{33}$$

$$k_6 = B_1 - A_1 B_0. \tag{34}$$

Figure 5 shows the block diagram of the digital implementation, and Figure 6 shows the output signals obtained by feeding the proposed model implemented using different $\omega(x)$ approximations and running at a sample rate of 44.1 kHz with the sum of two 2 V_{pp} sines of frequencies 110 and 150 Hz. We have set $V_T = 26$ mV, $I_s = 0.1$ fA, $R = 2.2$ kΩ, $C = 10$ nF.

Unlike the approaches outlined in [10], our method appears to be stable when using common discretization methods for all inputs of all amplitudes and using any of the approximations of $\omega()$ presented so far. Such a favorable outcome was not unexpected, since the explicit solution of the implicit model, even if approximate and in the discrete-time domain, necessarily relaxes the stiffness constraints of the problem. Indeed, similar results were obtained when modelling related circuits by approximate solutions in [17, 19, 20].

The audio-rate computational load consists of 5 sums, 9 multiplications, 1 sign function, and 1 $\omega()$ evaluation per sample. While we could not directly compare the computational requirements of our algorithm to those presented in [10] for the same circuit, its number of operations is so limited that it can be safely assumed to be suitable for real-time usage on all but the worst performing platforms.

5. CONCLUSIONS

This paper proposed the reformulation of expressions involving the main branch of the Lambert W function in terms of the Wright Omega function in the context of virtual analog modelling. Such an approach has the advantage of eliminating the computation of the exponential term typically found in the argument. Simple approximations of the Omega function have also been proposed that are well suited in real-time contexts where lower accuracy can be traded for lower computational load.

Such an approach was applied to model two example circuits, namely a common collector voltage buffer and a diode clipper, resulting in high quality and high performance digital implementations. In the latter case, the approximate solution of the implicit model in the discrete-time domain also allowed to greatly improve the stability of the algorithm w.r.t. previous models [10].

Implementations of the two applications examples (in MATLAB) and of the approximations of $\omega(x)$, $\log(x)$, and e^x (in C) are available at `http://dangelo.audio/dafx2019-omega. html`.

6. REFERENCES

[1] R. C. D. de Paiva, *Circuit modeling studies related to guitars and audio processing*, Ph.D. thesis, Aalto University, Espoo, Finland, 2013.

[2] S. D'Angelo, *Virtual analog modeling of nonlinear musical circuits*, Ph.D. thesis, Aalto University, Espoo, Finland, 2014.

[3] G. Borin, G. De Poli, and D. Rocchesso, "Elimination of delay-free loops in discrete-time models of nonlinear acoustic systems," *IEEE Transactions on Speech and Audio Processing*, vol. 8, no. 5, pp. 597–605, 2000.

[4] D. T. Yeh, J. S. Abel, and J. O. Smith, "Automated physical modeling of nonlinear audio circuits for real-time audio effects - Part I: Theoretical development," *IEEE Transactions on Audio, Speech, and Language Processing*, vol. 18, no. 4, pp. 728–737, 2010.

[5] A. Fettweis, "Wave digital filters: Theory and practice," *Proceedings of the IEEE*, vol. 74, no. 2, pp. 270–327, 1986.

[6] S. Petrausch and R. Rabenstein, "Wave digital filters with multiple nonlinearities," in *Proceedings of the European Signal Processing Conference*, Wien, Austria, September 2004, pp. 77–80.

[7] K. J. Werner, V. Nangia, Smith J. O., and J. S. Abel, "Resolving wave digital filters with multiple/multiport nonlinearities," in *Proceedings of the International Conference on Digital Audio Effects*, Trondheim, Norway, November 2015, pp. 387–394.

[8] W. Shockley, "The Theory of p-n Junctions in Semiconductors and p-n Junction Transistors," *Bell System Technical Journal*, vol. 28, no. 3, pp. 435–489, 1949.

[9] J. J. Ebers and J. L. Moll, "Large-signal behavior of junction transistors," *Proceedings of the IRE*, vol. 42, no. 12, pp. 1761–1772, 1954.

[10] D. T. Yeh, J. Abel, and J. O. Smith, "Simulation of the diode limiter in guitar distortion circuits by numerical solution of ordinary differential equations," in *Proceedings of the International Conference on Digital Audio Effects*, Bordeaux, France, September 2007, pp. 197–204.

[11] F. Fontana and M. Civolani, "Modeling of the EMS VCS3 voltage-controlled filter as a nonlinear filter network," *IEEE Transactions on Audio, Speech, and Language Processing*, vol. 18, no. 4, pp. 760–772, 2010.

[12] J. H. Lambert, "Observationes variae in mathesin puram," *Acta Helvetica*, vol. 3, no. 1, pp. 128–168, 1758.

[13] L. Euler, "De serie lambertina plurimisque eius insignibus proprietatibus," *Acta Academiae Scientiarum Imperialis Petropolitanae*, vol. 2, pp. 29–51, 1783.

[14] R. M. Corless, G. H. Gonnet, D. E. G. Hare, D. J. Jeffrey, and D. E. Knuth, "On the Lambert W function," *Advances in Computational Mathematics*, vol. 5, no. 1, pp. 329–359, 1996.

[15] T. C. Banwell and A. Jayakumar, "Exact analytical solution for current flow through diode with series resistance," *Electronics letters*, vol. 36, no. 4, pp. 291–292, 2000.
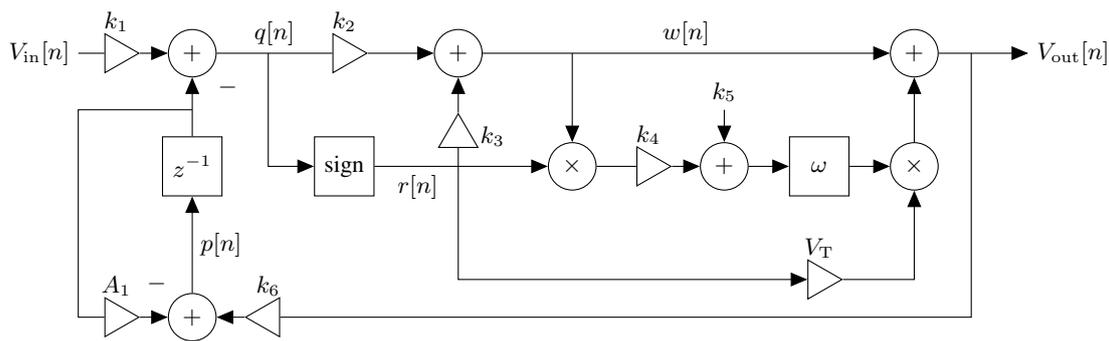
Figure 5: *Digital implementation of the diode clipper circuit.*

[16] J. Parker, "A simple digital model of the diode-based ring-modulator," in *Proceedings of the International Conference on Digital Audio Effects*, Paris, France, September 2011, vol. 14, pp. 163–166.

[17] R. C. D. Paiva, S. D'Angelo, J. Pakarinen, and V. Valimaki, "Emulation of operational amplifiers and diodes in audio distortion circuits," *IEEE Transactions on Circuits and Systems II: Express Briefs*, vol. 59, no. 10, pp. 688–692, 2012.

[18] J. Parker and S. D'Angelo, "A digital model of the Buchla lowpass-gate," in *Proceedings of the International Conference on Digital Audio Effects*, Maynooth, Ireland, September 2013, pp. 278–285.

[19] K. J. Werner, V. Nangia, A. Bernardini, J. O. Smith, and A. Sarti, "An improved and generalized diode clipper model for wave digital filters," in *Audio Engineering Society Convention 139*, New York, USA, October 2015.

[20] A. Bernardini, K. J. Werner, A. Sarti, and J. O. Smith, "Modeling nonlinear wave digital elements using the Lambert function," *IEEE Transactions on Circuits and Systems I: Regular Papers*, vol. 63, no. 8, pp. 1231–1242, 2016.

[21] F. Esqueda, H. Pöntynen, J. Parker, and S. Bilbao, "Virtual analog models of the Lockhart and Serge wavefolders," *Applied Sciences*, vol. 7, no. 12, 2017.

[22] D. A. Barry, J. Y. Parlange, L. Li, H. Prommer, C. J. Cunningham, and F. Stagnitti, "Analytical approximations for real values of the Lambert W-function," *Mathematics and Computers in Simulation*, vol. 53, no. 1-2, pp. 95–103, 2000.

[23] F. Chapeau-Blondeau and A. Monir, "Numerical evaluation of the Lambert W function and application to generation of generalized Gaussian noise with exponent 1/2," *IEEE Transactions on Signal Processing*, vol. 50, no. 9, pp. 2160–2165, 2002.

[24] D. Veberič, "Having fun with Lambert W(x) function," *arXiv preprint arXiv:1003.1628*, 2010.

[25] D. Veberič, "Lambert W function for applications in physics," *Computer Physics Communications*, vol. 183, no. 12, pp. 2622–2628, 2012.

[26] R. Iacono and J. P. Boyd, "New approximations to the principal real-valued branch of the Lambert W-function," *Advances in Computational Mathematics*, vol. 43, no. 6, pp. 1403–1436, 2017.

[27] F. N. Fritsch, R. E. Shafer, and W. P. Crowley, "Algorithm 443: solution of the transcendental equation $w * e^W = x$," *Communications of the ACM*, vol. 16, pp. 123–124, 1973.

[28] D. A. Barry, S. J. Barry, and P. J. Culligan-Hensley, "Algorithm 743: WAPR – a Fortran routine for calculating real values of the W-function," *ACM Transactions on Mathematical Software*, vol. 21, no. 2, pp. 172–181, 1995.

[29] R. M. Corless and D. J. Jeffrey, "The Wright ω function," in *Artificial intelligence, automated reasoning, and symbolic computation*, pp. 76–89. Springer, 2002.

[30] R. M. Corless and D. J. Jeffrey, "Complex Numerical Values of the Wright ω function," 2004, available online at http://www.orcca.on.ca/TechReports/2004/TR-04-04.html.

[31] P. W. Lawrence, R. M. Corless, and D. J. Jeffrey, "Algorithm 917: Complex double-precision evaluation of the Wright ω function," *ACM Transactions on Mathematical Software*, vol. 38, no. 3, pp. 20, 2012.

[32] D. Goldberg, "What every computer scientist should know about floating-point arithmetic," *ACM Computing Surveys*, vol. 23, no. 1, pp. 5–48, 1991.
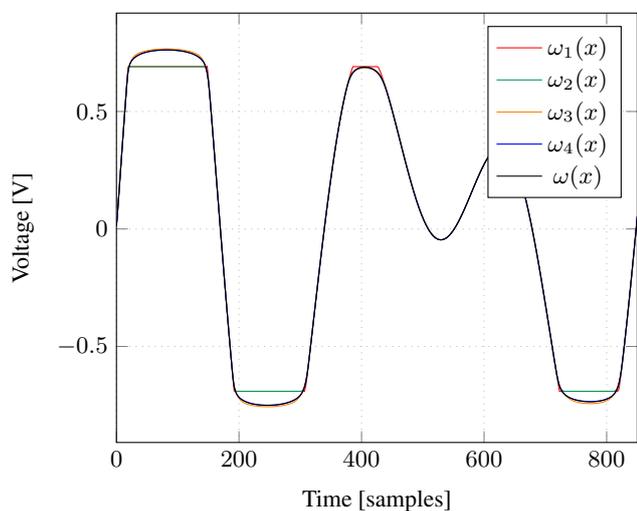
(a)
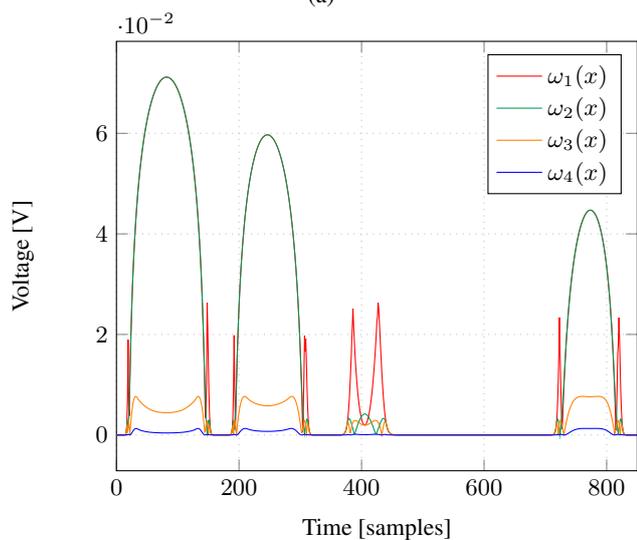
(b)

Figure 6: *Time domain waveforms (a) and absolute errors (b) of the output from the proposed diode clipper model implemented using the $\omega(x)$ approximations described in Section 3.1. The input is the sum of two 2 V$_{pp}$ sines of frequencies 110 and 150 Hz sampled at 44.1 kHz.*